Journal of Zhejiang University-SCIENCE A (Applied Physics & Engineering)
ISSN 1673-565X (Print); ISSN 1862-1775 (Online)
www.zju.edu.cn/jzus; www.springerlink.com
E-mail: jzus@zju.edu.cn

Influence of aerodynamic braking on the pressure wave of a crossing high-speed train*

Meng-ling WU†, Yang-yong ZHU, Chun TIAN, Wei-wei FEI

(*Research Institute of Railway & Urban Mass Transit, Tongji University, Shanghai 200092, China*)

†E-mail: wuml_sh@163.com

Received Sept. 23, 2011; Revision accepted Sept. 23, 2011; Crosschecked Sept. 26, 2011

Abstract: When aerodynamic braking works, the braking wings can change the flow field around the train, which may impact on the comfort and safety. Based on a sliding mesh, the pressure wave and flow field around high-speed trains with aerodynamic braking are analyzed. By comparing three typical intersection situations, the pressure wave of a high-speed train during braking (with or without aerodynamic braking) is studied. The analyses indicate that the pressure wave around the high-speed train body will change while using the aerodynamic braking, causing several pressure pulses on the surface of crossing high-speed trains. The distances between the pressure pulses are equal to the longitudinal distances of the brake wings, but the magnitudes of the fluctuations are less than those induced by the head of crossing trains. During the crossing, a train without aerodynamic braking will not impact the crossing train.

Key words: Aerodynamic braking, High-speed train, Crossing air pressure
doi:10.1631/jzus.A11GT011 **Document code:** A **CLC number:** U271.91

1 Introduction

Aerodynamic braking, as one of the non-adhesion braking methods, uses the pressure difference between two sides of the brake wing to generate resistance force by opening the braking wings on the roof. The force equivalent of the high-speed train braking force is proportional to the square of the velocity. As a result, this non-adhesion braking method functions very well under high speeds (Tian, 2006). At the same time, when aerodynamic braking works, the braking wings can change the flow field around the train. Some studies have shown that aerodynamic impulsion caused by crossing high-speed trains can result in serious impact on the comfort and safety (Wang, 2004; Qiu *et al*., 2005; Lu, 2006; Fei *et al*., 2009; Qi, 2010), including oversize deformation, loud noise, and windows being broken (Raghunathan *et al*., 2002; Tian, 2007). Therefore, this paper focuses on the characteristics of the pressure pulse of crossing high-speed trains.

Three typical cases of crossing events are studied and the air flow field and crossing air pressure waves for the three cases are simulated by the sliding mesh method in the computational fluid dynamics software FLUENT. By comparing the pressure waves of high-speed trains with or without aerodynamic braking, the influence of the braking system is determined.

2 Model of a high-speed train and grids partition

2.1 Geometric model of a high-speed train with aerodynamic braking

The calculation model of the train is a simplification model of the China Railway High-speed

* Project (No. 2009BAG12A05-13) supported by the National Key Technology R&D Program of China

(CRH) train, which is composed of the head, the tail, and six middle vehicles. Meanwhile, the model removes the protrusions of the train, so that the surface is smooth, and it also removes the complex components at the bottom of the train, so that there forms a slit between the train and the ground. The basic parameters of the train are shown in Table 1.

Table 1 Geometric parameters of the train

Parameter	Value (mm)
Length of the head (tail) vehicle	25 530
Length of the middle vehicle	24 175
Width of the vehicle	3255
Height of the vehicle	3680

The brake wings are installed on the train and operated as a rotary type. The brake wings are drawn back in the vehicle body when the train runs normally. The geometric appearance of the brake wings is shown in Fig. 1. Through numerical optimization calculation, we install seven couples of brake wings in the train, which is composed of eight vehicles. The brake wings distribute symmetrically among the longitudinal middle section of the train and the positions of the brake wings are shown in Fig. 2 (Fei *et al*., 2009).

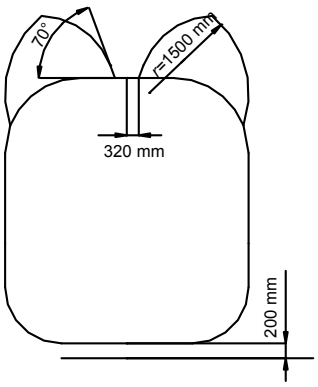

Fig. 1 Shape of the brake wing

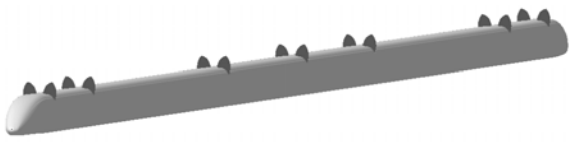

Fig. 2 Positions of the brake wings on the train (Fei *et al*., 2009)

2.2 Calculation area and the mesh partition

2.2.1 Selected section for the calculation area

We use the following calculation area: the length is 800 m, the width is 52.5 m, the height is 100 m, the track space is 5 m (Qi, 2010), and the slit between the bottom of the train and the ground is 0.2 m. The calculation begins when the distance between the two head vehicles is 50 m and then ends when the two tail vehicles are 50 m away. The calculation area is shown in Fig. 3.

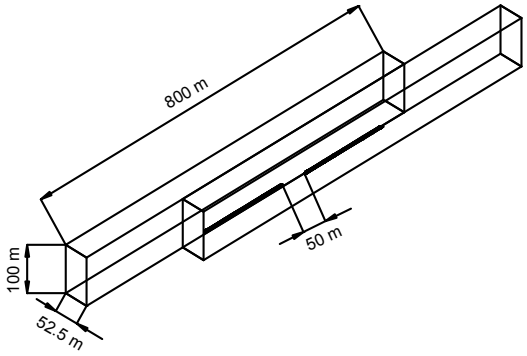

Fig. 3 Calculation area of the initial meeting time

2.2.2 Mesh partition of a single train

This study uses the ICEM CFD software to partition the structured mesh and adopts O-grid structure to partition the vehicle and the brake wing. The meshes are shown in Fig. 4. The mesh number of the single train with the brake wing is approximately 6.5 million, and without the brake wing is generally 5.5 million.

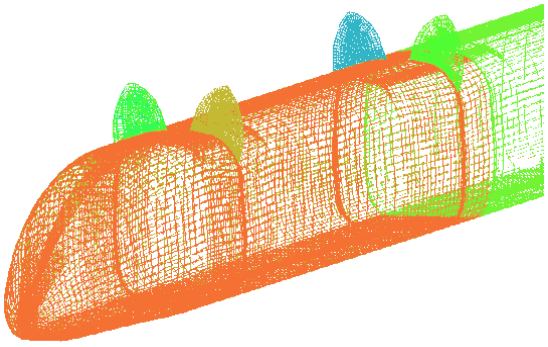

Fig. 4 Area meshes of the train and brake wings

2.2.3 Sliding mesh

The sliding mesh technology is adopted to exchange the mesh information between two trains, and the sliding mesh model allows the adjacent meshes to slide. We set the mesh area around the two trains to the sliding mesh type and then match the sliding velocity to the vehicle running speed before calculation. In order to simulate the real condition, we set a short calculation time step. However, the train is so long that the meeting time during the crossing process will be extended. Changing the unsteady time step is required to solve the problem; that is, we set the time step relatively long before the meeting time and relatively short during the meeting time. The long time step value is 0.018 s and the short one is 0.0045 s, which will not only shorten the calculation time, but also simulate the key points of the crossing process more closely.

There exists a border surface between the two train sliding meshes, and the border surface brings an internal area and two wall areas (Fig. 5). The overlap boundary surface area is the corresponding internal area. The number of pieces of border surface area varies due to the relative motivation of every boundary surface during the crossing process. The flow of the border surface will be calculated according to the face, which is born from the two boundary surfaces. The numerical simulation meshes that we adopt are shown in Fig. 6 and the mesh number is approximately 13 million.

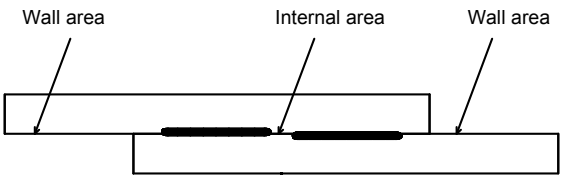

Fig. 5 Border area

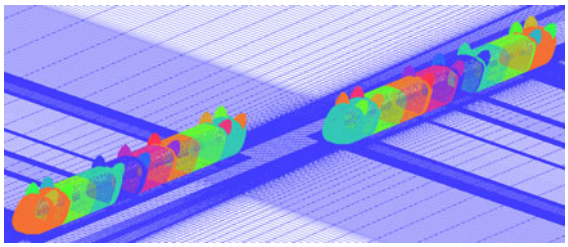

Fig. 6 Model of the meeting trains with brake wings

3 Numerical simulation of the aerodynamic status of crossing high-speed trains

According to the simulation model, the speed of the virtual high-speed train is 400 km/h. The study focuses on the characteristics of the flow field of crossing high-speed trains.

Condition 1: The crossing of two trains without aerodynamic braking.

Condition 2: The crossing of two trains, one with and one without aerodynamic braking.

Condition 3: The crossing of two trains with aerodynamic braking.

The crossing situation of two trains is shown in Fig. 7. The initial distance is set to be 50 m, and the trains are in the crossing period after 20 steps. On the 60th step, one train's head is passing the other's center. On the 148th step, the crossing period ends. Considering the influence of the wake flow of the trains, they keep on running until the distance between their tails is up to 50 m. The whole calculation process lasts 160 steps.

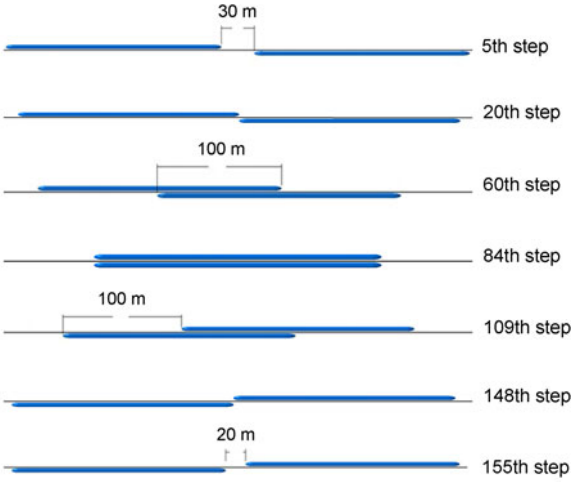

Fig. 7 Key moments during the crossing of high-speed trains

3.1 Characteristic of the air flow field

The following is the qualitative analysis of the flow field characteristics of a high-speed train with aerodynamic braking.

Fig. 8 shows different pressure contours on different steps of the crossing of high-speed trains. Comparing Figs. 8a and 8b, it is clear that the positive pressure areas on the windward surface of the brake

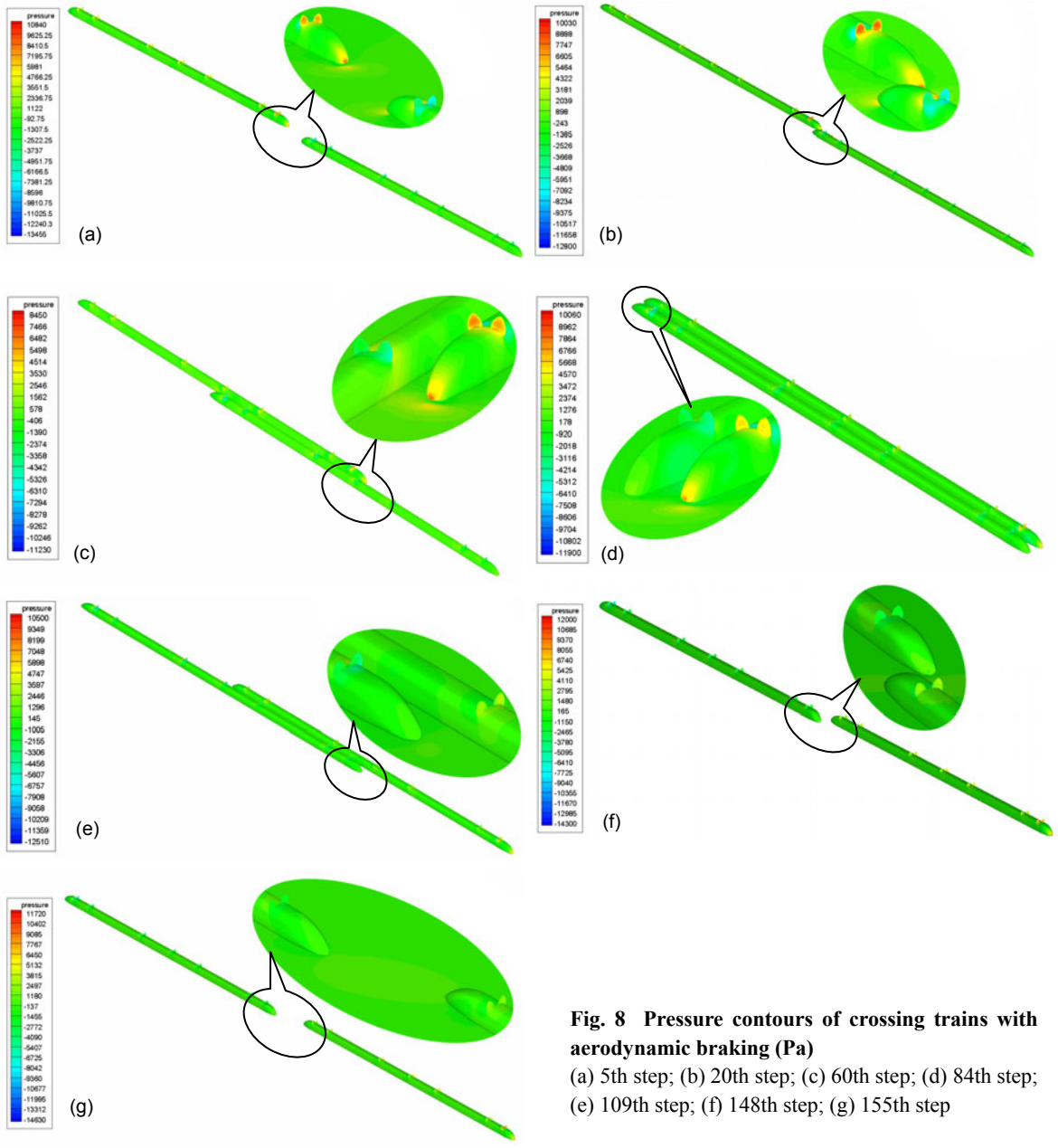

Fig. 8 Pressure contours of crossing trains with aerodynamic braking (Pa)
(a) 5th step; (b) 20th step; (c) 60th step; (d) 84th step; (e) 109th step; (f) 148th step; (g) 155th step

wing are enlarged, while the areas of negative pressure on the other side are also increasing. As shown in Fig. 8c, the pressure wave on one train's head can produce a positive pressure area on the other train's body. Similarly, the pressure waves around one train's brake wing can also cause similar positive pressure areas, which are depicted in Fig. 8e.

3.2 Influence of aerodynamic braking on the crossing train

The observation point is set on the surface of the train body near the 4th brake wing and is 2.5 m above the ground. The data of the observation point in conditions 1–3 with or without aerodynamic braking are compared.

In condition 1, as shown in Fig. 9, there are one positive and one negative pressure fluctuations around the observation points, which are in accordance with previous studies (Raghunathan *et al*., 2002).

The wave chart of the observation points in condition 2 is illustrated in Fig. 10. The pressure wave of the observation points on the high-speed train with

aerodynamic braking is similar to its counterpart in condition 1. However, the pressure wave on the other train indicates additional positive pressure fluctuation. Studying the moments of the occurrence of various pressure fluctuations, we can see that:

The 1st wave crest is on the 59th step when the head of one train is approaching the observation point.

The 2nd wave crest is on the 61st step when the 1st brake wing is near the observation point.

The 3rd wave crest is on the 64th step when the 2nd brake wing is near the observation point.

The 4th wave crest is on the 76th step when the 3rd brake wing is near the observation point.

The 5th wave crest is on the 82nd step when the 4th brake wing is near the observation point.

The 6th wave crest is on the 89th step when the 5th brake wing is near the observation point.

The 7th wave crest is on the 102nd step when the 6th brake wing is near the observation point.

The 8th wave crest is on the 105th step when the 7th brake wing is near the observation point.

The 9th wave crest is on the 109th step when the tail of the train is approaching the observation point.

We can see that distances between the pressure pulses are equal to the longitudinal distances of the brake wings. Thus, we can conclude that brake wings lead to the pressure pulses. In addition, Fig. 10 also shows that the amplitude of the pressure pulses caused by brake wings is far less than those at the head and the tail.

The wave chart of the observation points in condition 3 is illustrated in Fig. 11. As we can see from the figure, the pressure wave of the observation point on the high-speed train with aerodynamic braking is similar to its counterpart in condition 2. The pressure pulses of the observation points not only appear at the head and tail of the train, but also in the middle. During the crossing period, the highest crossing air pressure is 2 kPa. The glass of the train windows can endure 8.28 kPa (Qi, 2010), as glass is pasted to the windows, and it will not impact the safety when the track space is 5 m or more.

As shown in Figs. 9–11, if the crossing train is not equipped with aerodynamic braking, pressure pulses will not appear, except at the head and tail of the train. Thus, the train without aerodynamic braking will not impact the crossing train.

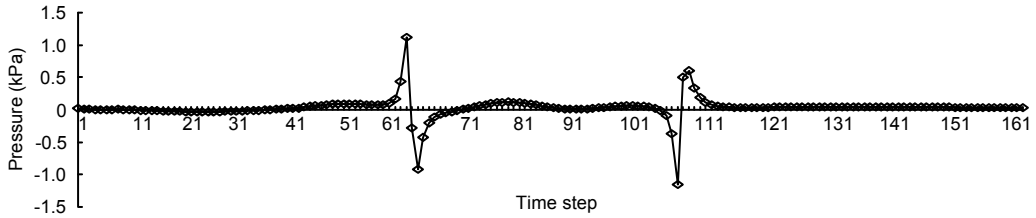

Fig. 9 Pressure waves of the observation point of the two trains without aerodynamic braking

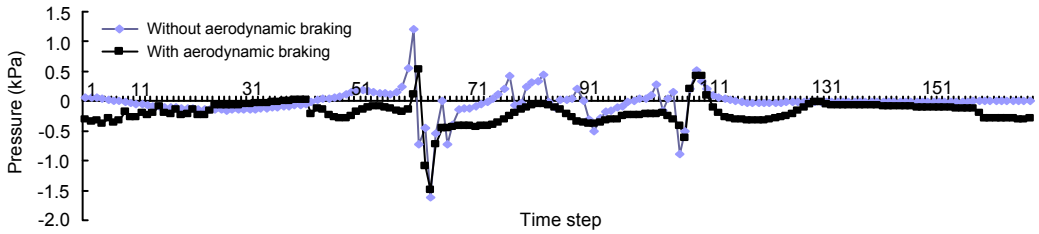

Fig. 10 Pressure waves of the observation point of the two trains with and without aerodynamic braking

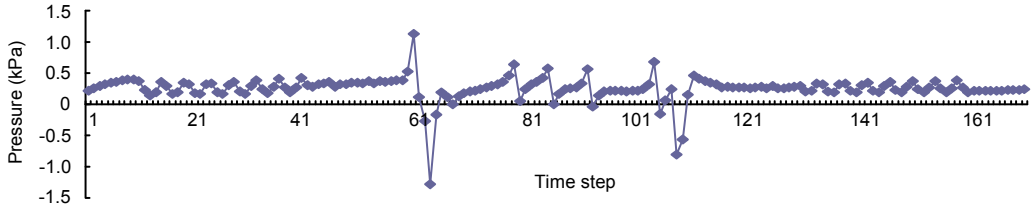

Fig. 11 Pressure waves of the observation point of the two trains with aerodynamic braking

4 Conclusions

Three typical cases in the crossing events are studied and the air flow field and crossing air pressure wave under the three cases are simulated by the sliding mesh method in the computational fluid dynamics software FLUENT. By comparing the pressure waves of high-speed trains with or without aerodynamic braking, the influence is determined. The result shows that:

1. When two trains with aerodynamic braking pass by each other, the highest crossing air pressure is 2 kPa.

2. When a train passes by another one equipped with aerodynamic braking, the air pressure pulse around the train head will cause a positive low pressure area. Analogously, the air pressure pulse around the brake wing will cause a pressure-oscillation area on the surface of the train body.

3. When two trains equipped with aerodynamic braking pass by each other, the pressure pulses of observation points not only appear at head and tail of the train, but also in the middle. The middle pulses result from the brake wings. And the amplitude of the pressure pulses caused by brake wings is far less than those at the head and the tail.

4. If the crossing train is not equipped with aerodynamic braking, pressure pulses will not appear except at the head and tail of the train. Thus, a train without aerodynamic braking will not impact the crossing train.

References

Fei, W.W., Tian, C., Wu, M.L., 2009. Research on Brake Type of High-Speed Train Based on Air Dynamics. The National Industrial Aerodynamic Academic Conference, Changsha, China, p.238-244 (in Chinese).

Lu, G.D., 2006. The aerodynamics points of high speed trains. *Rolling Stock*, **44**(6):1-3, 44-45 (in Chinese).

Qi, Z.D., 2010. Aerodynamics Research on High-Speed Train Passing Each Other. MS Thesis, Southwest Jiaotong University, Chengdu, China (in Chinese).

Qiu, Y.Z., Xu, Y.G., Wang, Y.L., 2005. An Aerodynamic Model of Bottom Structures of High-Speed Trains. Fluent Chinese User Conference, p.151-155 (in Chinese).

Raghunathan, R.S., Kim, H.D., Setoguchi, T., 2002. Aerodynamics of high speed railway train. *Progress in Aerospace Sciences*, **38**(6-7):469-514. [doi:10.1016/S0376-0421(02)00029-5]

Tian, H.Q., 2006. Study evolvement of train aerodynamics in China. *Journal of Traffic and Transportation Engineering*, **6**(1):1-9 (in Chinese).

Tian, H.Q., 2007. Train Aerodynamics. China Railway Press, Beijing, China (in Chinese).

Wang, F.J., 2004. Computational Fluid Dynamics (CFD) Software Analysis Principle and Application. Tsinghua University Press, Beijing, China, p.67-70 (in Chinese).